Utilizing the conventional, object-oriented and pixel-based techniques to estimate erosion and sediment yield by MPSIAC model

Panah Mohamadi[1], Abbas Ahmadi[2†], Bakhtiar Feizizadeh[3], Ali Asghar Jafarzadeh[4], Mehdi Rahmati[5]

[1] Ph.D. graduate [2] Associate Professor [4] Professor, Department of Soil Science, University of Tabriz, Tabriz, Iran
[3] Associate Professor, Department of Remote Sensing and GIS, University of Tabriz, Iran
[5] Associate Professor, Department of Soil Science and Engineering, University of Maragheh, Iran Institute of Bio- and Geosciences: Agrosphere (IBG-3), Forschungszentrum Jülich GmbH, 52425 Jülich, Germany

†*Corresponding Author Email*: A_ahmadi@tabrizu.ac.ir

Abstract

Soil erosion and sediment yield in the downstream areas, water transfer canals, and dams are the most serious problems in the world today. Soil erosion threatens soil resources, causes severe damage to infrastructures, and imposes high costs on agriculture, watershed management, and natural resources. Reducing these hazards and damages due to soil erosion and sediment yield requires the use of quantitative data to identify critical areas that require immediate protection. Due to the high cost and time consuming of conventional methods, the use of new remote sensing technologies and satellite imagery is essential. This study used the MPSIAC model, one of the most well-known models for estimating soil erosion and sediment yield in Iran, geographical information system (GIS), and satellite image processing with object-oriented and pixel-based methods. For this purpose, basic data were prepared using base maps, Sentinel-2 satellite imagery, meteorological and hydrometric data, and fieldwork. After establishing a database, the score for each of the nine factors of the MPSIAC model was determined using the three common, object-oriented, and pixel-based processing methods. The extent of soil erosion and sediment yield of the watershed was determined within each hydrologic unit. Based on the results, the soil erosion and sediment yield intensities of the Lighvan watershed were classified as medium class (III). However, the comparison of the specific soil erosion and sediment yield values obtained from the three methods showed that the use of object-oriented methods in determining the values for land cover, land use, and current soil erosion state increased the accuracy of the predictions (with the estimated error of 12.18% and 13.15% for sediment yield and erosion, respectively) compared to common (with the estimated error of 15.73% and 16.71%) and pixel-based (with the estimated error of 18.78% and 19.45%) methods.

Keywords: object-oriented, pixel-based, remote sensing, Satellite image, MPSIAC model.

1. Introduction

Soil, as the most valuable natural resource of any country, has always been seriously threatened by erosion. Soil erosion is a widespread problem of land degradation and has irreversible effects on the economy, the environment, natural ecosystems, and human life (especially in arid and semi-arid regions). Sediment yield caused by this process not only leads to water pollution, but also causes dams to fill up and reduce the productivity potential of land, environment, and natural resources (Zandi, 2012). Soil erosion leads to nitrogen and phosphorus runoff through the loss of fertile topsoil, resulting in water pollution (Di Stefano et al., 2016; Hancock et al., 2015; Tanyas et al., 2015). Several studies have shown that several different factors such as climate change, land use, and land cover play an extremely important role in soil erosion (Li et al., 2016; Diyabalanage et al., 2017; Ganasri and Ramesh, 2016; Zhang et al., 2017). For this reason, it is necessary to identify the factors that affect it and implement the necessary prevention and management measures (Razavi

et al., 2015).

Although numerical models are used to study and predict soil erosion and sediment yield, existing models vary in complexity when it comes to understanding and estimating soil erosion from field data collected with remote sensing equipment and geographic information systems (GIS) (Fernandez et al., 2003; Xu et al., 2009).

The main problem is that these models require detailed and large numbers of data. However, most watersheds lack sufficient data and hydrometric stations (Merritt et al., 2003; Nigel, 2010). Therefore, it is important to use alternative and less costly methods, such as zonation methods, to predict and assess soil erosion. On the other hand, modeling physical and dynamic processes such as soil erosion is fraught with problems and errors. The lack of availability of accurate data sources, the quality of the data used, scale problems in modeling, measurement errors, and model complexity are among the problems cited by many researchers in soil erosion studies (Erfanian et al., 2015).

Nowadays, due to the great variety of effective

factors identified in the soil erosion process and the need for different, fast, and accurate analysis of information, it is possible to obtain satellite images using remote sensing techniques and database formation in a GIS environment and their analysis to provide all the necessary quantitative parameters in erosion models (Lidmaza, 2004). The main advantages of the MPSIAC model are the quantification of the sediment yield and the consideration of the largest number of effective factors for soil erosion. The MPSIAC model predicts soil erosion based on nine factors, including geologic features, soil, climate, runoff, topography, vegetation cover, land use, current soil erosion, and stream bank erosion (PSIAC, 1968). MPSIAC is believed to be suitable for environmental conditions in Iran (Bagherzadeh, 1993; Sadeghi, 1993).

Remote sensing and GIS are advanced systems for natural resource studies (Feizizadeh et al., 2020), especially for studies on soil erosion and sediment yield in watersheds (Lin et al., 2002; Qiao and Qiao, 2002; Sahin and Kurum, 2002; Martinez-Casasnovas, 2003). Due to the time and cost savings and more accurate results than conventional methods, they have been widely used by researchers and used as a powerful and cost-effective tool in various studies (Holbling et al., 2015). In addition, many advances in computer science and artificial intelligence have led to the development of new techniques. One of these techniques is object-oriented analysis, which automatically extracts natural objects from satellite imagery (Feizizadeh and Salmani, 2016; Feizizadeh et al., 2017; Feizizadeh et al., 2018; Batz et al., 2000). In fact, the object-oriented analysis method is one of the most important classification methods for extracting information from satellite imagery. In this method, the desired effects are identified based on the spectral, morphological, and contextual features of the object and using expert knowledge (Brodaski et al., 2006).

Spectral similarities of various phenomena on the Earth's surface and the resulting interference in the classification of satellite images required the use of spatial and environmental information such as compactness, shape, location, pattern, etc. This important requirement was realized by processing object-oriented satellite images (Blashaki et al., 2014). In the object-oriented method, the images are segmented based on the spectral, physical, and geometric parameters of the ground phenomena recorded on the image, and the image processing units are changed from pixels to image phenomena or segments. As a result of this change, information processing became more comprehensive and object extraction more accurate (Feizizadeh et al., 2007). This technique was performed as an iterative process by performing the steps of image segmentation, training data extraction, feature space optimization, and selection of appropriate classification algorithms in the

eCognition software to obtain the highest membership level for each of the visual objects. Finally, each of the visual objects should be assigned to one (or none) of the classes (Feizizadeh and Salmani, 2016; Feizizadeh et al., 2009; Abedi et al., 2015). Considering the possibility of simultaneous review of all the required parameters in erosion and sediment yield studies, using conventional methods is time-consuming and costly, on the other hand, the lack of accurate and quantitative data, Researchers have turned to using new methods and up-to-date data to speed up their analyzes and increase the accuracy of their analyses. Currently, new techniques have greatly helped to improve the qualitative and quantitative levels of studies in the agriculture field. Therefore, the objective of the study was to evaluate object-oriented and pixel-based processing techniques for soil erosion and sediment prediction and mapping using the empirical MPSIAC model in the Lighvan watershed, northwest of Iran.

2. Materials and methods
2.1. Study area

The study area was Lighvan watershed (between latitudes 37º 45' 00" N to 37º 50' 00" N and longitudes 46º 25' 00" E to 46º 26' 00" E). The Lighvan watershed, with an area of 76 km^2 and a perimeter of 42.13 km is located on the northern slope of the Sahand Mountains, East Azerbaijan Province, Iran (Figure 1). For homogenizing the working area, the watershed was divided into 13 units (Figure 2) based on the DEM, slope, hydrology, geological, and vegetation maps using ArcGIS and the eCognition software.

2.2. MPSIAC model and conventional method of evaluating the factors

The MPSIAC model uses an aggregation of scores for nine different factors including geologic features, soil, climate, runoff, topography, vegetation cover, land use, current soil erosion, and stream bank erosion to predict soil erosion and sediment yield (Table 1) (PSIAC, 1968). These required data and maps were obtained from the National Cartographic Center of Iran, the Regional Water Company of East Azerbaijan, and the hydrological station of the basin. In addition, field assessments were conducted to identify the natural characteristics of the watershed, adjust the available maps of the study area, identify the current soil erosion types, assess the condition of vegetation, and take ground control points using GPS. To this end, regional erosion and sediment yield reports were prepared during fieldwork in the study area; and erosion status and types were studied in the units of the watershed. Soil samples (135 samples from the surface layer of the soil) were collected for laboratory testing and characteristics of soil samples (soil texture, bulk density, percentage of organic matter and calcium carbonate equivalent, EC, pH, and SAR) were measured.

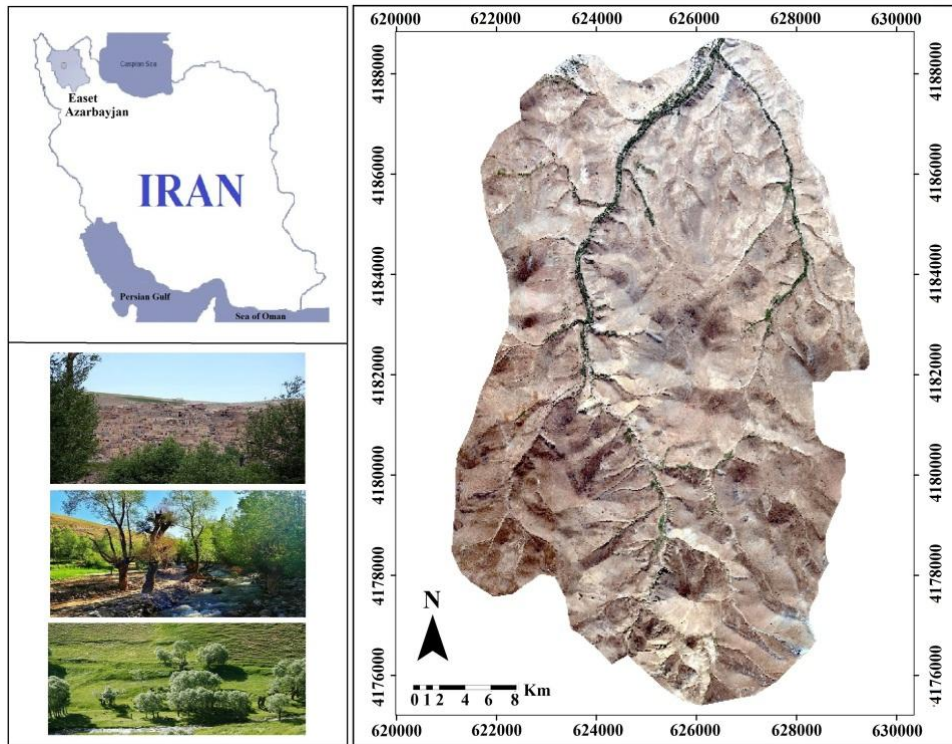After determining the point values for all factors, the

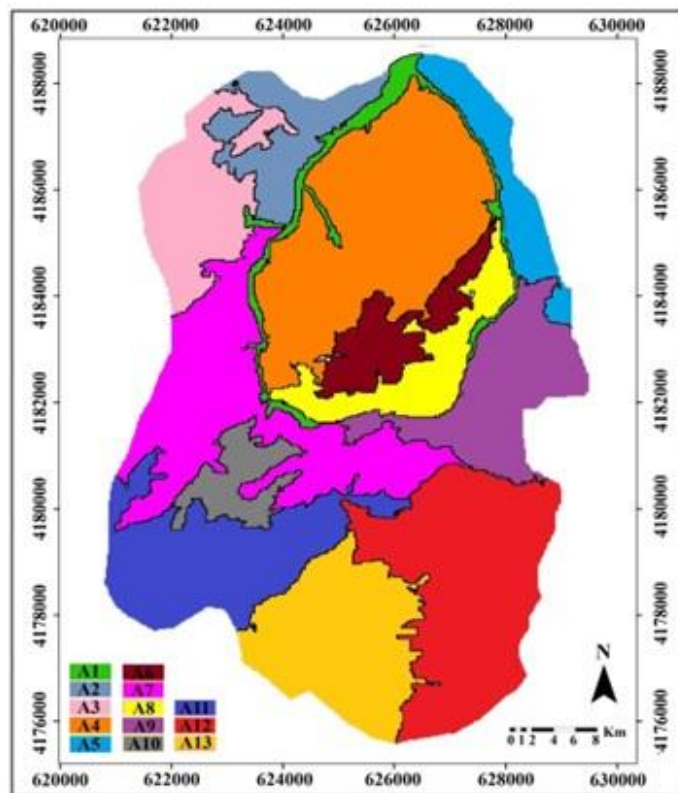**Fig 1.** Location of the Lighvan watershed in East Azerbaijan Province, Iran.

Fig 2. Segments of working units.

Table 1. Factors used for the MPSIAC model with the descriptions and scoring functions.

Factors	Equation	Domain of value	Description
Surface geology	$Y_1 = X_1$	0 to 10	X_1 determined based on stone type hardness and fracture
Soil	$Y_2 = 16.67X_2$	0 to 10	X_2 is the soil erodibility factor in the USLE model
Climate	$Y_3 = 0.2X_3$	0 to 10	X_3 is 6-h rainfall intensity with a returning period of 2 years (mm)
Runoff	$Y_4 = 0.006R + 10Q_P$	0 to 10	R is annual runoff elevation (mm), and Q_p is specific peak discharge measured ($m^3s^{-1}year^{-1}$)
Topography	$Y_5 = 0.33X_5$	0 to 20	X_5 is the average slope (%)
Land cover	$Y_6 = 0.2X_6$	-10 to 10	X_6 is the bare grounds at each land unit (%)
Land use	$Y_7 = 20 - 0.2P_c$	-10 to 10	P_c is the canopy covering each land unit (%)
Current state of erosion	$Y_8 = 0.25\,S.S.F$	0 to 25	S.S.F is the score of soil surface erosion in the BLM model
Gully erosion	$Y_9 = 1.67\,S.S.F.g$	0 to 25	S.S.F.g is the score of gully erosion in the BLM model

Table 2. Parameters layer weights used for the segmentation processes in this study

Parameter	Scale	Shape	Compactness	Slope	DEM	Bands 2 to 8 Sentinel-2 images
Layer Weight	50-70	0.6-0.7	0.3-0.4	0.0	0.0	1.0

sediment yield for each unit was calculated using the following equation:

$$Q_s = 38.77e^{0.0353R} \qquad [1]$$

where Q_s is sediment yield (m^3/ km^2 year) and R is sediment yield rate, which is the sum of the scores for the nine effective factors in sediment yield prediction by the MPSIAC model.

Equations 2 and 3 were used to calculate the sedimentation delivery ratio (SDR):

$$Log\,SDR = 1.877 - 0.142 \times Log\,S \qquad [2]$$

$$SDR = \frac{SY}{E} \qquad [3]$$

where SDR is the sedimentation delivery ratio (one square mile) and *S* is the area of the working unit of the watershed (in square miles), SY is the sediment yield (m^3 km^{-2} yr^{-1}) at the watershed outlet, and E is the total soil loss (m^3 km^{-2} yr^{-1}), defined as the total eroded soil on the lands eroding above the watershed outlet. Once the sediment yield of the study area is determined, Table 2 can be used to classify the study area based on its sediment yield production capability.

2.3. Research scenarios

The MPSIAC model-required scores of three factors including land cover, land use, and current erosion state were evaluated using field campaigns and available maps and filling the scoresheets by user (known as conventional method) as well as using satellite imagery applying object-oriented and pixel-based image processing algorithms. The scores for the remaining factors were determined using the conventional methods as explained in the MPSICA user manual. Finally, the accuracy of the erosion and sediment predictions for these three different scenarios were subjected to statistical analysis. Figure 3 illustrates the steps taken for sediment mapping in the study area.

2.4. Satellite images

MSI-Sentinel-2 satellite imagery (August 23, 2016) was used to assess the land cover, land use, and current erosion condition (surface erosion) factors. During initial preprocessing, the Sentinel-2 satellite images were atmospherically corrected and georeferenced using SNAP software (Mueller et al., 2016). They were analyzed and processed using ERDAS, ArcGIS, and eCognition.
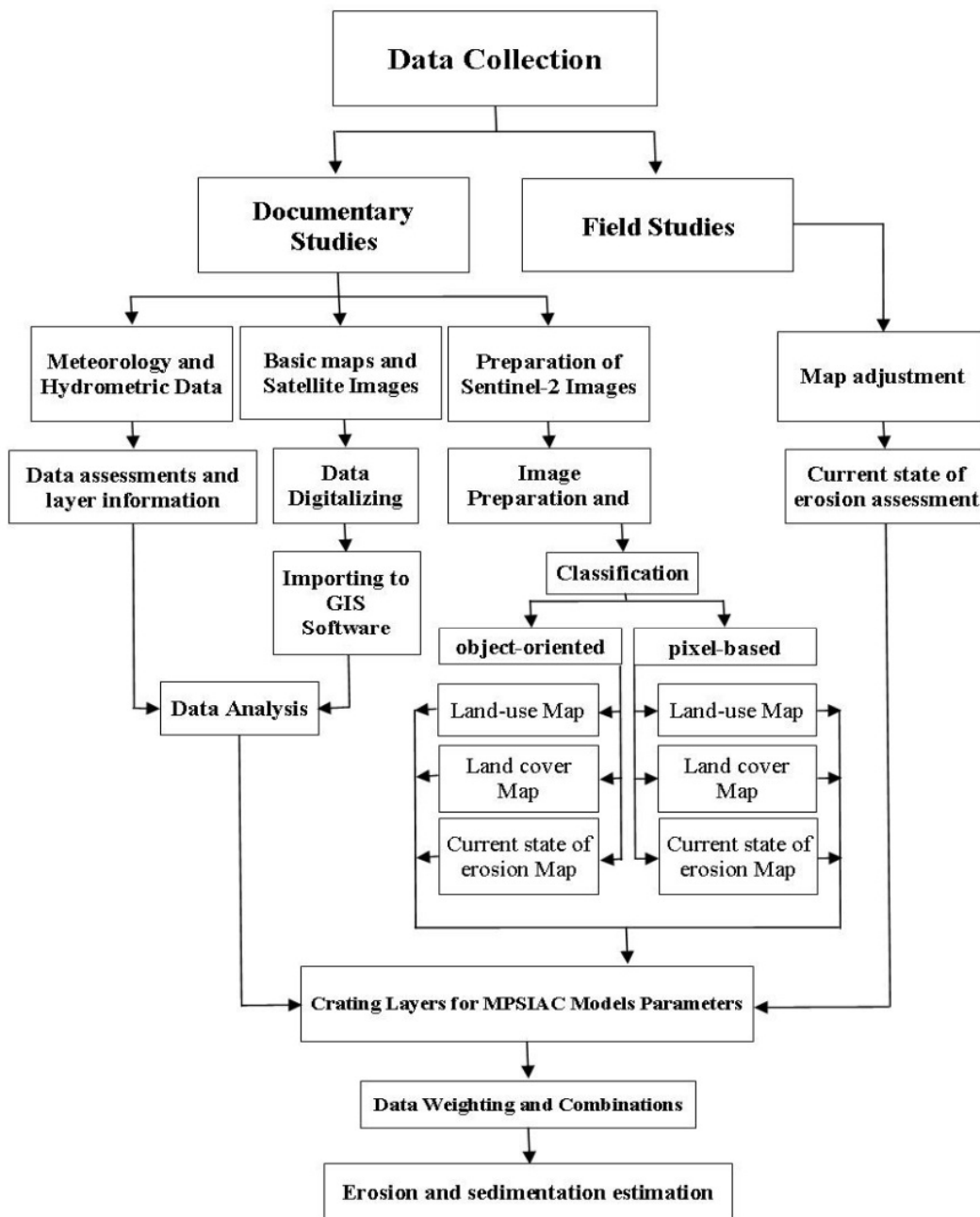
Fig 3. Flowchart of the sediment yield estimation through the MPSIAC model

2.5. Pixel-Based Image Analysis

In the image processing phase, we first performed detection functions and then image classification based on basic pixel methods (Feizizadeh et al., 2016). In digital remote sensing images, each pixel has a specific numerical value that reflects the spectral behavior of the corresponding phenomenon on the ground. By analyzing the numerical values of the digital images, it is possible to identify and classify terrestrial features (land cover, land use, and current erosion state) on the image. This type of classification based on the numerical value of pixels, where phenomena with the same numerical value are classified into a group, is called basic pixel classification (Feizizadeh and Helali, 2009).

In order to pixel base images analyze, we used the evaluation of correlations among the bands, the band composition from 2 to 8 in the Sentinel-2 images was selected and used together with DEM, geology, and slope layers for classification and detection. In the next step,
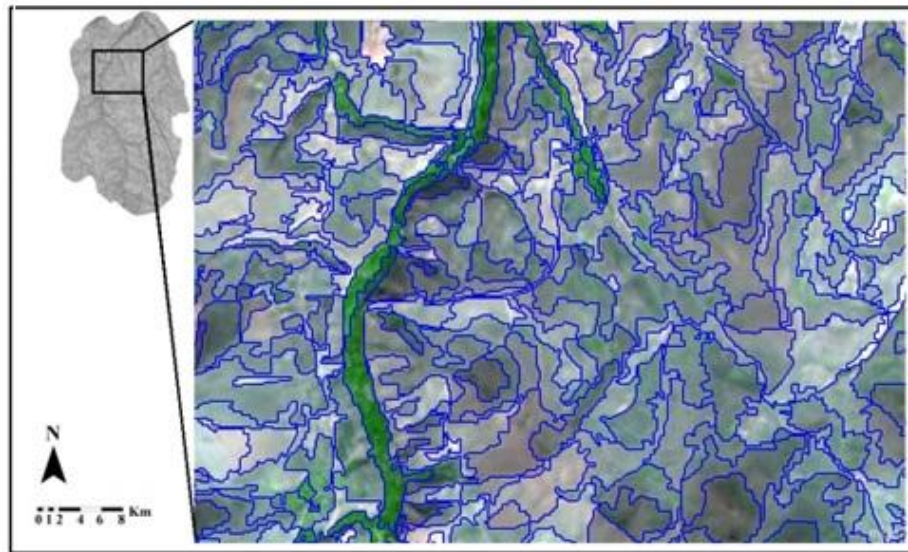
117

Fig 4. Segmentation map of Lighvan watershed with multiresolution algorithm (scale size 100)

using training patterns generated based on collected data with GPS, through field sampling, pixel base classification was done. For this purpose, the training patterns were implemented on the image processing software and the resolution of the classes was calculated by extracting the features in terms of their spectral and statistical signs. Finally, the spectral features of the cases were known sufficiently, classification was performed based on the base pixel algorithm.

2.6. Object-Based Image Analysis (OBIA)

Image segmentation is performed using various algorithms such as multiresolution, Chessboard, Quadtree, and Contrast Split Segmentation. In this study, bands 2 to 8 of Sentinel-2 images along with DEM and slope layers were selected and different scaling parameters (10 to 100) and shape and compactness coefficients (total equal to one) were defined in the eCognition software. Then, the segmentation process is performed with different methods by trying the scaling parameters and heterogeneity weighting of the softness and compactness parameters and comparing the results of each of them. Finally, the multiresolution segmentation method was selected as the most suitable method for this step of image processing (Figure 4).

The visual objects resulting from the segmentation process are the basis of object-oriented classification. Since they have many features corresponding to terrestrial phenomena, this directly affects the quality of the object-oriented classification (Feizizadeh, 2017). For these reasons, segmentation parameters (including scale, shape, and compactness) for each of the erosion classes (surface, rill, and gully),the vegetation, and land use classes were selected for segmentation of the image using

the multiresolution segmentation method, and the degree of homogeneity and compatibility of the created segment with the training samples was evaluated. Finally, the most appropriate dimensions of the visual objects with the effects in the image were selected as segmentation dimensions for detection and classification (Table 2).

Object-oriented classification is a reproducible process based on fuzzy techniques. In this process, identified segments are evaluated according to the degree of membership to the specified classes and are classified into the class with the highest degree of membership (Faizizadeh, 2017). Thus, after classification, each image object is assigned to one (or none) of the classes. By determining the features in terms of spectral information and geometric properties, fuzzy logic operators are also used in this research, including AND, ALP, OR, MAR, MGE, and MGEW (Aksoy and Ercanoglu, 2012), and by training the system with training data (sampling with field operations and recording their spatial information with GPS), we defined the appropriate conditions for classification in the eCognition software. It should be noted that to compare the results of the methods used in this research (object-oriented and pixel-based), a common training dataset was used for both methods.

3. Results and Discussion

In this study, three different scenarios were used to evaluate the required factors of the MPSIAC model to predict soil erosion and sediment yield in the Lighvan watershed in northwestern Iran. Table 3 shows the scores for these factors from the different scenarios and the final values for the soil erosion and sediment yield predictions. According to the results presented in Table 3, the summation of the scores factors (R) of the whole

Table 3. The scores for factors in the MPSIAC model in the study area and its working units.

working units	Area (ha)	Surface geology	Soil	Climate	Runoff	Topography	Land cover a	b	c	Land-use a	b	c	Current state of erosion a	b	c	Chanel erosion	R a	b	c	Qs (tons/ha/year) a	b	c
				5.0	2.43		3.00	3.04	3.33	4.00	4.12	4.71	7.25	5.50	6.50	3.34	42.51	40.92	42.70	1.14	1.07	1.14
A2	233	6.6	5.4	5.0	2.43	6.13	5.67	5.92	5.91	8.45	5.92	8.84	11.50	11.25	10.75	8.35	59.53	57.00	59.41	2.07	1.89	2.06
A3	536	5.6	5.3	5.0	2.43	5.39	5.16	4.84	5.47	7.86	7.29	8.25	14.25	11.50	12.75	13.36	64.35	60.71	63.55	2.45	2.16	2.38
A4	1238	6.0	4.3	5.0	2.43	5.87	5.15	4.94	5.04	7.73	7.34	7.58	13.75	13.00	14.00	16.70	66.93	65.58	66.92	2.69	2.56	2.69
A5	302	6.3	3.3	5.0	2.43	5.48	5.24	4.74	5.30	8.02	7.15	7.90	11.75	11.25	10.00	13.36	60.88	59.01	59.07	2.17	2.03	2.04
A6	277	6.0	5.3	5.0	2.43	7.16	5.28	5.40	5.30	7.71	7.79	7.66	7.75	8.75	8.75	8.35	54.98	56.18	55.95	1.76	1.84	1.82
A7	971	4.2	5.3	5.0	2.43	7.45	5.08	5.19	5.31	7.73	7.68	7.73	16.50	13.25	13.25	18.37	72.06	68.87	71.04	3.22	2.88	3.11
A8	351	5.4	4.9	5.0	2.43	6.35	5.02	5.37	5.09	7.43	7.63	7.44	13.75	11.25	11.25	20.04	70.32	68.37	69.90	3.03	2.83	2.98
A9	573	6.3	6.6	5.0	2.43	6.17	5.30	5.14	5.48	8.15	7.99	8.51	10.75	7.75	7.75	13.36	64.06	60.74	64.10	2.43	2.16	2.43
A10	214	4.3	4.9	5.0	2.43	8.65	5.09	5.88	5.48	7.54	8.56	7.96	12.50	8.25	8.25	15.03	65.44	63.00	63.75	2.55	2.34	2.40
A11	739	4.1	3.7	5.0	2.43	6.93	4.95	5.71	5.18	7.49	8.02	7.52	10.50	7.50	7.50	18.37	63.47	61.76	62.98	2.38	2.24	2.34
A12	1046	4.1	4.0	5.0	2.43	6.85	5.18	5.56	5.28	7.83	7.87	7.71	18.00	17.00	17.00	16.70	70.09	69.51	69.57	3.01	2.94	2.95
A13	717	3.3	3.3	5.0	2.43	7.06	5.04	5.61	5.23	7.76	8.27	7.74	17.50	16.75	16.75	16.70	68.09	68.42	67.26	2.81	2.83	2.72
Watershed	7476	5.1	4.4	5.0	2.43	6.54	5.10	5.26	5.23	7.68	7.70	7.72	12.75	11.00	11.00	1397	62.97	61.40	62.33	2.34	2.21	2.28

a: the conventional method, b: the object-oriented method, c: the pixel-based method

Table 4. Determination of the annual sediment yield and erosion classes in the MPSIAC model

Erosion class	Qualitative classification	Sediment Yield	Sedimentation Intensity
		m³/km² yr	%
V	Very High	>1450	100-150
IV	High	450-1450	75-100
III	Moderate	250-450	50-75
II	Low	95-250	25-50
I	Very low	<95	0-25

watershed was 62.97 and the annual sediment yield was 2.34 tons/ha/year. The comparison of the annual sediment yield obtained by the conventional estimation method of the MPSIAC model (scenario a) with the values obtained by the object-oriented (scenario b) and pixel-based (scenario c) methods (2.21 and 2.28, respectively) shows that the use of remote sensing, especially the object-oriented method, can be a good alternative to the conventional scoring method of MPSIAC model. This is because the use of the remote sensing method not only saves the cost and time of fieldwork, but also provides the opportunity to conduct comprehensive and continuous studies in time series (Alavipanah, 2012; Ramachandra et al., 2004). Eliminating researchers' errors in assessment, usually through personalization, also increases the accuracy of estimates. The values obtained for the three factors (land cover, land use, and current erosion status) were compared.

Using Eq. 1 and the values given in Table 3, sediment yield was predicted for the study area and its working units. Finally, the predicted sediment yield was classified into different classes using Table 4 (Refahi, 2017).

According to the standard sediment yield grade classification matrix (Table 4), the entire watershed is classified as a medium class, and working units A1 and A7 with minimum and maximum sediment yield were classified as low and high sediment yield classes, respectively. Table 5 shows a comparative plot of sediment yield in the Lighvan watershed based on the three methods used in this study. The erosion rate of the watershed is the main target of erosion and sediment yield studies. However, since some of the eroded soil sediment yields on the surface of the watershed during transport out of the watershed and does not reach the sediment yield and hydrometric stations, the amount of eroded soil calculated at the stations is less than the actual amount. Therefore, the amount of sediment yield calculated at the station is less than the actual amount of eroded soil from the watershed. In this study, to accurately estimate the amount of erosion, the specific erosion was determined and then the total erosion was estimated by this factor.

After analyzing and evaluating 9 factors affecting

erosion, sediment yield intensity and one class thereof in each working unit were determined, and the area and percentage of the area of each class in each of the working units of the watershed were calculated (Table 5). The erosion and sediment yield classes of the watershed studied were classes II and III, which have low and medium sedimentation intensity, respectively.

Working unit A1, which covers 2.55% of the total study area, was classified as sedimentation intensity class II, and the erosion rate is low. The vegetation in this unit is in good condition, and most of it is covered by agricultural land and gardens. In this regard, this unit had the lowest values of 3, 3.04, and 3.33 for land cover factor and 4, 4.12, and 4.71 for land use factor based on the scores of the three methods used in this study (conventional method (a), object-oriented method (b), the pixel-based method (c), respectively) (Table 5). Accordingly, the amount of erosion and resulting sediment yield in this unit is the lowest compared to the other units (a=1.14, b=1.07, and c=1.14 t/ha/year). The highest amount of erosion and produced sediment yield occurs in unit A7 (a=3.32, b=2.88, and c=3.11 t/ha/y), which covers 12.99% of the total study area. This is followed by units A8 and A12 with the highest amounts of production sediment yield. These three classes, together with the other classes (except for class A1) were classified as erosion and sediment yield group III. This covers a total of more than 97% of the study area. It can be concluded that erosion and sediment yields are so severe in these areas that the implementation of soil and water conservation programs is necessary and a priority and the use of these areas is very limited.

According to the results in Table 5, the amounts of specific erosion and sediment yield calculated for the Lighvan catchment were compared. According to this table, the amount of specific erosion in the catchment calculated by the conventional method (a) is larger than that calculated by the other two methods, object-based (b) and pixel-based (c), and the object-based method accounts for the lowest calculated amount. The amount of special sediment yield estimated by the above methods is equal to the magnitude of special erosion. In other words, the two methods using satellite image processing to evaluate the MSPAC factors and estimate the specific

Table 5. Specific erosion and sediment yield in the watershed and each working unit

Working units	Area ha	Area %	SDR	sediment yield tons/ha/year a	b	c	sediment yield ton/year a	b	c	Erosion tons/ha/year a	b	c	Erosion ton/year a	b	c	Erosion and sedimentation class
A1	189	2.55	0.44	1.14	1.07	1.14	214.43	202.73	215.87	2.59	2.45	2.61	490.15	463.39	493.45	II
A2	323	4.35	0.49	2.07	1.89	2.06	668.27	611.18	665.45	4.21	3.85	4.19	1359.34	1243.19	1353.59	II
A3	526	7.05	0.54	2.45	2.16	2.38	1290.12	1134.56	1254.19	4.54	3.99	4.41	2385.69	2098.03	2319.27	II
A4	1238	16.58	0.65	2.69	2.56	2.69	3325.97	3171.19	3324.79	4.16	3.97	4.16	5151.29	4911.57	5149.48	III
A5	302	4.05	0.48	2.17	2.03	2.04	655.32	613.46	614.76	4.50	4.21	4.2	1359.39	1272.55	1275.26	III
A6	277	3.71	0.47	1.76	1.84	1.82	488.06	509.18	505.06	3.72	3.88	3.85	1030.72	1075.32	1066.62	III
A7	971	12.99	0.61	3.22	2.88	3.11	3126.53	2793.56	3015.96	5.24	4.68	5.06	5092.26	4549.94	4912.17	III
A8	351	4.70	0.49	3.03	2.83	2.98	1062.86	992.16	1047.22	6.09	5.68	5.99	2137.19	1995.02	2105.74	III
A9	573	7.67	0.55	2.43	2.16	2.43	1391.08	1237.24	1393.05	4.41	3.92	4.42	2527.20	2247.72	2530.77	III
A10	214	2.88	0.45	2.55	2.34	2.40	545.47	500.45	513.88	5.68	5.21	5.35	1215.18	1114.89	1144.81	III
A11	739	9.89	0.58	2.38	2.24	2.34	1757.11	1654.18	1726.97	4.09	3.86	4.03	3028.33	2850.93	2976.39	III
A12	1046	13.99	0.62	3.01	2.94	2.95	3141.76	3078.09	3084.62	4.82	4.72	4.73	5038.83	4936.71	4947.18	III
A13	717	9.59	0.58	2.81	2.83	2.72	2006.78	2030.29	1948.84	4.85	4.91	4.71	3480.35	3521.13	3379.86	III
Watershed	7476	100	0.54	2.34	2.21	2.28	17464.55	16522.98	17074.41	4.36	4.13	4.26	32610.91	30852.75	31882.42	III

a: the conventional method, b: the object-oriented method, c: the pixel-based method

Table 6. Comparison of estimated erosion and sediment yield with MPSIAC model and measured data at Lighvan watershed

Parameter	measured	MPSIAC model		
		usual method	object-oriented method	pixel-based method
Specific sediment yield (ton/ha/year)	1.97	2.28	2.21	2.34
Total sediment yield (ton/year)	14727.72	17074.4	16522.9	17464.6
specific soil erosion (ton/ha/year)	3.65	4.26	4.13	4.36
Total soil erosion (ton/year)	27273.55	31882.5	30852.8	32610.9

Table 7. Percentage of the estimation error of estimated parameters compared with measured

Parameter	MPSIAC model		
	usual method	object-oriented method	pixel-based method
Specific sediment yield (ton/ha/year)	15.73	12.18	18.78
specific soil erosion (ton/ha/year)	16.71	13.15	19.45

erosion and sediment yield have lower estimated values than the conventional method.

3.1. Evaluation of the accuracy of estimation

After estimating the specific erosion and sediment yield of the Lighvan watershed using the MPSIAC model, the results were evaluated and compared with the measured sediment yield and erosion amounts in the hydrometric station of the Lighvan watershed to evaluate the applicability of this model to compare the three evaluation methods (conventional method, object-oriented method, and pixel-based method), which is shown in Table 6.

Table 7 shows that the specific erosion and sediment yield values estimated by the MPSIAC model differ slightly from the measured values at the Lighvan hydrometric station. Of course, all three methods used for estimation (conventional method, object-oriented method, and pixel-based method) overestimated specific erosion and sediment yield compared to the measured one. The overestimation rate of the above methods was evaluated according to Equation 4, and its amount for each of the estimation methods is shown in Table 7.

$$OV = \left(\frac{Es - Me}{Me} \right) * 100 \qquad [4]$$

Where OV is the percentage of estimation error, Es is the amount of estimated sediment yield and soil erosion, and Me is the measured sediment yield and soil erosion.

Table 7 shows that the amount of specific sediment yield determined by the MPSIAC model (using all three methods) was overestimated. The object-oriented method estimated both the specific erosion and sediment yield parameters more accurately (the estimation error is

12.18% and 13.15%, respectively). While the pixel basis method has the highest estimation error (the estimated error is 18.78% and 19.45%, respectively). In other words, the object-oriented method reduces the estimation error by about 6%. This error reduction in the object-oriented method is about 3% compared to the conventional method. Thus, the object-oriented method estimated both the specific erosion and sediment yield parameters more accurately than both the conventional and pixel-based methods.

4. Conclusion

In this study, the MPSIAC model and the remote sensing and satellite image processing method were used. For the evaluation of three out of nine factors of the model (land cover, land use, and current erosion condition) the conventional, pixel-based, and object-oriented methods were utilized. The results showed that the use of remote sensing while reducing the cost of field studies and saving time, increased the accuracy of the estimation of erosion and sediment yield in the object-oriented method (about a 3% reduction in the estimation error compared to the conventional method). However, when using the pixel-based method, the accuracy of the soil erosion and sediment yield estimates decreased being 3% higher than the conventional method. This decrease in accuracy probably is due to using only the numerical value of pixel spectral information in image classification, which is eliminated and reduced in the new object-oriented method due to the use of other information such as texture, shape, position, and content in the classification process that in consequence increases the degree of image classification accuracy and the accuracy of the estimations (Blaschke et al., 2014; Feizizadeh et al., 2017). In other words, geometric features as one of the

most important algorithms of object-oriented processing led to better results in extracting maps of land use, land cover, and the current state of erosion from satellite imagery. The results of this study confirm the superiority of the object-oriented method over the traditional pixel-based method in classifying satellite imagery, and show that comparing different classification techniques and identifying the most efficient object-oriented algorithms for evaluating each of the nine factors of the MPSIAC model can speed up erosion and sediment yield investigations and save time and cost.

Based on the results obtained from the use of the object-oriented method in the analysis of satellite images, and increasing the accuracy and speed of MPSIAC model estimation, it is suggested that the use of satellite images with high resolution and accuracy, along with the use of object-oriented processing method, given more attention by researchers in the studies related to soil science, especially soil erosion and sediment yield.

Availability of data and materials

The datasets generated and/or analyzed in the current study are available upon request from the corresponding author.

Conflict of Interests

The authors declare no conflict of interest.

References

Alavi-panah, S. K. (2012). *Application of Remote Sensing in the Earth Sciences (soil)*. 4th Edition. Tehran: University of Tehran Press. (In Persian).

Baatz, M., & Schape, A. (2000). Multiresolution Segmentation: an optimization approach for high quality multi scale image segmentation, In: Strobl, L.J. Blaschket. and Griesebener T. (Eds), Angewandte geographische informationseraabeitung XII, Beitrage zun AGIT Symposium Salzburg. *Herbert Wichmann Verlag, Heidelberg*, 5(3), 12-23.

Bagherzadeh, M. (1993). *A Study on the Efficiency of Erosion Potential and Sediment Yield Models Using Remote Sensing and Geographic Information Systems*. Unpublished M.Sc. Thesis, Natural Resources College, University of Tarbiat Modares, Tehran, Iran (In Persian).

Blaschke, T., Feizizadeh, B., & Holbling, D. (2014). Object-Based Image Analysis and Digital Terrain Analysis for Locating Landslides in the Urmia Lake Basin, Iran. *IEEE Journal of Selected Topics in Applied Earth Observerion and Remote Sensing*, 7(12), 4806 – 4817. https://doi.org/10.1109/JSTARS.2014.2350036

Di Stefano, C., Ferro, V., Burguet, M., & Taguas, E. V. (2016). Testing the long-term applicability of USLE-M equation at an olive orchard micro catchment in Spain. *Catena*, *147*, 71-79.

Diyabalanage, S., Samarakoon, K. K., Adikari, S. B., & Hewawasam, T. (2017). Impact of soil and water conservation measures on soil erosion rate and sediment yields in a tropical watershed in the Central Highlands of Sri Lanka. *Applied Geography, 79*, 103-114.

Fizizadeh, B. (2018). A Novel Approach of Fuzzy Dempster–Shafer Theory for Spatial Uncertainty Analysis and Accuracy Assessment of Object-Based Image Classification. *IEEE Geoscience and Remote Sensing Letter*s, *15*(1), 18-22.

Feizizadeh, B., & Salmani, S. (2016). Modeling Agricultural Destruction Lands Resulted by Urban Growing in Suburb of Urmia City by Applying an Object Based Image Analysis Approach. *Journal of Town and Country Planning, 8*(2), 177-202. (In Persian).

Feizizadeh, B., Blaschke, T., Tiede, D., & Rezaei Moghaddam, M. (2017). Evaluating fuzzy operators of an object-based image analysis for detecting landslides and their changes. *Geomorphology, 293*, 240-254.

Feizizadeh, B., Kazamei, M., Blaschke, T., & Lakes, T. (2020). An object-based image analysis applied for volcanic and glacial landforms mapping in Sahand Mountain, Iran. *Catena*, *198*, 1-19. https://doi.org/10.1016/j.catena.2020.105073.

Feizizadeh, B., Zand Karimi, A., Pirnazar, M., & Abedi, H. (2015). Evaluating the Capability of Fuzzy algorithms for Improving the Accuracy of land use maps Based on object based image analysis. *Journal of geographic information sciences, 24*, 107-117.

Fernandez, C., Wu, J. Q., McCool, D. Q., & Stockle, C. O. (2003). Estimating water erosion and sediment yield with GIS, RUSLE and SEDD. *Journal of Soil Water Conservation, 58*(3), 128-136.

Ganasri, B. P., & Ramesh, H. (2016). Assessment of soil erosion by RUSLE model using remote sensing and GIS - A case study of Nethravathi Basin. *Geoscience Front, 7*, 953-961.

Ghaderi, A., Najmaei, M., & Azizifar, V. (2010). *Assessment and analysis of erosion and sediment Shahid Rajaei dam's watershed using remote sensing and GIS technologies and MPSIAC model*. The first regional conference of Civil Engineering. Ghaemshahr, Iran.

Hancock, G. R., Wells, T., Martinez, C., & Dever, C. (2015). Soil erosion and tolerable soil loss: insights into erosion rates for a well-managed grassland catchment. *Geoderma, 237-238*, 256-265.

Razavi, M. M., Biniaz, M., Asadi, A., & Ajza Shokouhi, M. (2015). Estimation of soil erosion and deposit generation in Bekr Abad drainage basin in Varzghan using MPSIAC in GIS environment. *Geographical Space, 15*(49), 237-257.

Holbling, D., Friedl, B., & Eisank, C. (2015). An object-based approach for semi-automated landslide changes

detection and attribution of changes to landslide classes in northern Taiwan. *Earth Science Informatics, 8*(2), 327-335.

Li, T., Liu, K., Ma, L. Y., Bao, Y. B., & Wu, L. (2016). Evaluation on soil erosion effects driven by land use changes over Danjiang River Basin of Qinling Mountain. *Journal of Natural Resources. 31*(4), 583-595 (in Chinese with English abstract).

Lin, C. Y., Lin, W. T., & Chov, W. C. (2002). Soil erosion prediction and sediment yield estimation: the Taiwan experience. *Soil Tillage Research, 68*, 143-152.

Erfanian, M., Ghahramani Saatloo, P., & Saadat, H. (2015). Assessment of soil erosion risk using a fuzzy model in Gharnaveh Watershed, Golestan. *Journal of Water and Soil Conservation, 21*(6), 135-154.

Martinez–Casasnovas, J. A. (2003). A spatial information technology approach for the mapping and quantification of gully erosion. *Catena, 50*(2–4), 293-308.

Merritt, W. S., Letcher, R. A., & Jakeman, A. J. (2003). A review of erosion and sediment transport models. *Environmental Modelling and Software, 18*, 761-799.

Mueller, U., Devignot, O., & Pessiot, L. (2016). MPC Sen2Cor Configuration and User Manual. S2-PDGS-MPCL2A-SUM-V2.3 Issue: 01.

Nigel, R., & Rughooputh, S. D. D. V. (2010). Soil erosion risk mapping with new dataset: An improved prioritization of high erosion risk area. *Catena, 82*(3), 191-205.

Qiao, Y. L., & Qiao, Y. (2002). Fast soil erosion investigation and dynamic analysis in the Loess Plateau of China by using information composite technique. *Advance Space Research, 29*(1), 85-88.

PSIAC. (1968). Report of the water management subcommittee on factors affecting sediment yield in the pacific southwest area and selection and evaluation of measures for reduction of erosion and sediment yield.

Refahi, H. G. (2017). *Water Erosion and Conservation*, 7th edn. University of Tehran, 672 Pages.

Sadeghi, H. (1993). *Comparison of some erosion potential and sediment yield assessment models in Ozon-Dareh subcatchment.* Proceedings of the National Conference on Land Use Planning, Tehran, Iran.

Sahin, S., & Kurum, E. (2002). Erosion risk analysis by GIS in environmental impact assessments: a case study—Seyhan Köprü Dam construction. *Journal of Environ Manage, 66*(3), 239-247.

Shabanlou, S. (2010). *Prediction of the erosion and sediment of the Golestan catchment Using MPSIAC model and GIS technology.* The first Conference of Applied Research in Water Resources, 405-420.

Tanyas, H., Kolat, Ç., & LütfiSüzen, M. (2015). A new approach to estimate cover-management factor of RUSLE and validation of RUSLE model in the watershed of Kartalkaya dam. *Journal of Hydrology, 528*, 584-598.

Xu, Y. Q., Shao, X. M., & Peng, J. (2009). Assessment of soil erosion using RUSLE and GIS: a case study of the Maotiao River watershed, Guizhou Province, China. *Environmental Geology, 56*, 1643-1652.

Zandi, J. (2012). *Prioritization of controlling area on soil erosion using RS and GIS techniques (A case study: Vzaroud watershed, Mazandaran).* M.Sc. Thesis. Faculty of Natural Resources. Sari Agricultural and Natural Resources University 144 pages.

Zhang, S. H., Fan, W. W., Li, Y. Q., & Yi, Y. J. (2017). Influence of changes in land use and landscape patterns on soil erosion in a watershed. *Science of the Total Environment, 574*, 34-45.